Published in final edited form as:
Magn Reson Imaging. 2011 January ; 29(1): 19–24. doi:10.1016/j.mri.2010.07.005.

Anterior Cingulate and Cerebellar GABA and Glu Correlations measured by ^{1}H J-Difference Spectroscopy

Kevin W. Waddell[1,2], **Parham Zanjanipour**[10], **Subechhya Pradhan**[1,2,3], **Lei Xu**[4], **Edward B. Welch**[1,2], **James M. Joers**[1,2], **Peter R. Martin**[5,6], **Malcolm J. Avison**[1,2,5,7], and **John C. Gore**[1,2,3,8,9]

[1] Institute of Imaging Science, Vanderbilt University, Nashville, Tennessee

[2] Department of Radiology and Radiological Sciences, Vanderbilt University, Nashville, Tennessee

[3] Department of Physics and Astronomy, Vanderbilt University, Nashville, Tennessee

[4] Department of Biostatistics, Vanderbilt University, Nashville, Tennessee

[5] Department of Pharmacology, Vanderbilt University, Nashville, Tennessee

[6] Department of Psychiatry, Vanderbilt University, Nashville, Tennessee

[7] Department of Neurology, Vanderbilt University, Nashville, Tennessee

[8] Department of Molecular Physiology and Biophysics, Vanderbilt University, Nashville, Tennessee

[9] Department of Biomedical Engineering, Vanderbilt University, Nashville, Tennessee

[10] Department of Medicine, University of Kentucky, Lexington Kentucky

Abstract

Gamma-aminobutyric acid (GABA) and glutamate (Glu) levels, normalized to total creatine (tCr) were measured in the anterior cingulate and cerebellar vermis in healthy adults (n=19, age = 24.6 +/ 6.4 yrs) using ^{1}H MRS at 3 Tesla and metabolite correlations across regions and subjects were determined. Mean anterior cingulate and cerebellar GABA:tCr ratios were 0.31 (0.08) and 0.23 (0.06), respectively, while corresponding Glu levels were 1.16 (0.10) and 0.70 (0.07), respectively. A correlation was observed for glutamate ($r = 0.61$, $p = 0.01$ and $p = 0.06$ when adjusted for multiple comparisons) between the anterior cingulate and the cerebellar vermis. It is unlikely that this correlation is driven by correlations in tCr, since inter-regional correlations were not observed for other metabolites referenced to tCr. Within both regions, correlations were observed between metabolites which were also weakly significant when correcting for multiple comparisons. N-acetyl-aspartate and glutamate (anterior cingulate: $r = 0.66$, $p = 0.01$ and $p = 0.06$ when adjusted for multiple comparisons; cerebellar vermis: $r = 0.64$, $p = 0.01$ and $p = 0.06$ when adjusted for multiple comparisons).

Address Correspondence to: Kevin Waddell, Ph.D., Vanderbilt Institute of Imaging Science, Vanderbilt University, 1161 21st Avenue South, Medical Center North, AA-1105, Nashville, TN 37232-2310, Phone: (615)343-8019, Fax:(615)322-0734, kevin.waddell@vanderbilt.edu.

Keywords

gamma-aminobutyric acid; GABA; glutamate; anterior cingulate; cerebellar vermis; J-Difference; MRS; metabolite correlations

Introduction

Dysfunctional signaling in the anterior cingulate (AC) and cerebellar vermis (CV) is associated with a variety of neuropsychiatric and neurological disorders. Lesions in either region have canonical effects; in the AC these include deficits in attention, error detection and conflict resolution as well as emotional effects (1), whereas CV damage is more often associated with errors in movement and motor learning. In addition to the effects of local insult, both regions have been implicated in the pathophysiology of some disorders. For example, functional imaging studies indicate that disrupted anterior cingulate function is a hallmark of many substance use disorders (2), and, as a proxy for cerebellar development, infant motor development has been found to predict propensity for alcoholism in adulthood (3).

The events that precede clinical manifestations of disorders associated with these areas may have corresponding regional neurotransmitter alterations that are accessible by ^{1}H magnetic resonance spectroscopy (MRS). In particular, the major inhibitory and excitatory neurotransmitters, GABA and glutamate, respectively, can be measured with sufficient SNR and spectral resolution to afford measurement precision less than 10%. Although these important neurochemicals can be measured *in vivo*, they have been reported sparsely in tandem in the AC and CV because their concentrations are low and near threshold detection levels. Where these compounds have been reported, the spectral appearance has frequently been inconsistent with prior-knowledge of the spin-systems. Hence, more data are needed to establish the relative abundance and correlation of these neurotransmitters and metabolites in the AC and CV in normal subjects.

Human brain metabolites have been previously measured in the AC and CV by at least three techniques: tissue biopsy, autopsy, and in-vivo ^{1}H MRS. When compared to ^{1}H MRS, biopsy and autopsy measurements have high sensitivities using established analytical chemical methods, albeit with the caveat that the in-vitro chemical profiles may differ from their *in vivo* counterparts. In particular, it has been shown that GABA levels depend on the delay between extraction and measurement, and this is likely to be true in general due to persistent and differential post-mortem enzymatic activity (4,5).

From predominantly gray matter samples obtained by biopsied and autopsied cerebral cortex, GABA (including homocarnosine and lysine) to Glu ratios have been found to be 0.13 and 0.32, respectively, while cerebellar counterparts were 0.20 and 0.41 (6). Ratios of these amino acids from autopsied samples are elevated due to the relative postmortem increases in GABA versus Glu (4,5). For both autopsy and biopsy, cerebral cortex and lateral cerebellar samples were taken from predominantly gray matter (GM). In contrast to these types of studies, where neurochemicals from several brain regions have been directly extracted and analyzed, human *in vivo* GABA concentrations measured by MRS techniques that are capable of measurement precisions less than 10% are infrequent in the literature.

In order of descending frequency, localized GABA measurements have been reported in the occipital lobe (7,8), parieto-occipital (9–11), frontal cortex (9,10), and the substantia nigra (12), but regionally paired measurements of GABA and Glu have not been reported. There is considerable variation in measurement methodology, post-processing, contaminant

correction, concentration referencing, tissue specificity, and spectral quality among these reports. Nevertheless, GABA levels appear approximately two-fold higher in the substantia nigra relative to the prefrontal, parietal, and occipital cortex, where reported values are clustered around 1 umol/g. Voxel dimensions were anatomically limited in the substantia nigra, and in the other areas, study volumes were 27 (4) mL.

We have measured GABA+ (GABA + co-edited compounds) and Glu with respect to a total creatine (tCr) reference in 19 healthy volunteers in order to better understand normative GABA+ and Glu levels in the AC and CV, and also characterized associated interregional correlations and measurement reproducibility of all metabolites that were present above the sensitivity threshold (Cramer-Rao Lower Bounds < 10%). In particular, this study addresses two primary goals: 1) to determine mean values and variance for GABA and Glu and 2) to investigate intra and inter-regional correlations of these metabolites across subjects which may be helpful for establishing a basis from which to better understand disorders involving concerted effects spanning the anterior cingulate and the cerebellar vermis.

Methods

19 healthy volunteers (11 females and 8 males, age = 24.6 +/ 6.4 yrs) participated in this study, and all protocols were in accordance with procedures approved by the Vanderbilt University Institutional Review Board.

Imaging

Anatomical images for spectroscopy voxel planning were acquired using an RF-spoiled 3D inversion-prepared T1-weighted turbo field echo (TFE) sequence running on a Philips X-series Achieva 3.0 T whole body MR scanner (Philips Healthcare, Best, Netherlands) with the standard 30.0 cm diameter T/R coil. Key parameters of the sequence were: acquired voxel size = 0.9 mm × 0.9 mm × 0.9 mm; field of view size = 230 mm × 230 mm × 171 mm; number of slices = 190; TR/TE=6.7/3.1 milliseconds; flip angle = 8 degrees; inversion delay time = 900 milliseconds; inversion interval = 3 seconds; sampling bandwidth = 241.4 hertz/pixel (water-fat shift = 1.8 pixels); TFE factor = 256; acquisition time = 12 minutes 8 seconds. Sagittal planes were acquired to increase scan efficiency and the isotropic data sets were reformatted into coronal and axial orientations for improved voxel planning.

Spectroscopy

To achieve maximum SNR and resolution, a previously described acquisition and postprocessing quality control algorithm was used in these experiments (13). These procedures are critical for minimizing deleterious impacts on spectral quality due to susceptibility-induced frequency and phase variations. In addition, acquisition parameters were optimized for measurement of glutamate from difference spectra.

256 and 384 phase-cycled transients were acquired and stored separately in memory from AC (7.32 mL) and CV (6.10 mL) volumes, respectively, using the MEGA-PRESS localized J-difference spectroscopy sequence (14) with 2.5 second recycle delays, 2048 complex points, 73 ms echo-time, and 2 kHz receiver bandwidth. Selective inversions were achieved with 15.64 ms sinc (center lobe) pulses (64 Hz FWHM), and these were applied at 1.91 ppm on odd numbered acquisitions and at a position symmetric about the water resonance on even numbered acquisitions. The carrier frequency was maintained within ~2 Hz using the manufacturer navigator frequency drift compensation option. A 140 Hz sinc-gauss water suppression pulse (15) and four outer volume suppression slabs preceded localization. Radiofrequency power and shim settings were optimized automatically using the standard Philips spectroscopy preparation routine.

Post-processing

The acquired arrays of frequency toggled (odd/even scans) and phase-cycled free induction decays (FIDs) were processed automatically using a two step algorithm to remove phase and frequency variations, as previously described (13). Briefly, the starting fit estimates (with amplitude scaled appropriately) were obtained by fitting the summed FIDs to the real part of a Lorentzian time-domain function using global nonlinear least squares. Individual FIDs were subsequently determined in a more tightly constrained but otherwise identical time-domain fitting procedure.

Quantification

After correcting for frequency and phase variations, a 2 Hz exponential filter was applied to the time-domain signals to suppress noise in the tail of modestly over-sampled FIDs. The J-difference (odd - even acquisitions) and the even acquisitions (standard PRESS) were then extracted and analyzed with LCModel (16). Using the GAMMA library, basis sets for prior-knowledge fitting were generated from metabolite density matrix simulations employing ideal slice selection and 64 Hz sinc inversion pulses. Simulated FIDs were summed from 10,000 points in a magnetic field gradient to account for the differential impact of crusher gradients in the presence of the spectrally selective inversion pulses. Since J-difference spectral baselines are well behaved, LCModel baselines were maximally constrained for difference spectra. GABA, Glu, and NAA were quantified from the J-difference data, while NAA was also quantified from the standard PRESS acquisitions, enabling referencing of the entire metabolite set to total creatine.

Statistical Methods

The data set contains repeated measures and has an unbalanced design. To estimate the mean concentration ratio we fit a linear mixed effect model separately for each metabolite using the restricted maximum likelihood (REML) method. Subject factor was included as a random effect to account for the correlation between repeated measurements. We checked the model assumption using residual plots and no severe violation was found. The inter-region and intra-region correlations between pairs of metabolites were estimated using the weighted correlation coefficient between subject means (16). A total of 25 correlations were calculated. To adjust for multiple comparisons, we adopted the false discovery rate (FDR) method (17), which controls the expected proportion of incorrectly rejected null hypotheses. Both raw and adjusted p-values are reported.

Results

Representative AC and CV spectra from healthy normal adults (n = 19, 8 males and 11 females, 24.6 +/− 6.4) are shown in Figure 1 and 2; individual spectra were consistent with prior-knowledge of the metabolite spin-systems (see Methods) (18). The consistency of acquired spectra is illustrated in Figure 3, where individual AC spectra were automatically summed. The resolution and spectral appearance of these composite data mirror the individual acquisitions. The edited pseudo-doublet resonances from GABA+ at 3.01 ppm were clearly resolved in all cases, and resonances from a combination of Glu, glutamine, and glutathione at ~3.75 ppm along with co-edited macromolecules (19) at 0.9 ppm were also consistent with prior knowledge and demonstrate well-behaved baselines (Figure 2). Mean Cramer-Rao lower bounds (CRLBs), which are proportional to nominal lower limits of precision, ranged from 7 for AC GABA to 2 for CV tCh (data not shown), and SDs (Table 1) were similar but uniformly greater than calculated lower bounds.

A range of CRLBs have been used in the literature to validate metabolite quantifications, with a 15 % cutoff commonly chosen. However, a 10 % cutoff was invoked in this study

because metabolites at or below this level were readily discerned by visual inspection, while at more liberal cutoffs, metabolites such as aspartate, glutamine and glutathione were fit without conspicuous spectral counterparts.

The resolution and qualitative metabolite constitution of AC and CV volumes were similar, but signal to noise (SNR) was generally higher in the AC acquisitions (Figure 1), where volumes were 17 % larger and acquisitions 66 % shorter. The relative abundance of tCr with respect to other prominent singlet resonances (NAA and tCh) was markedly higher in cerebellar volumes. The SNR of GABA and tCr in the AC was approximately 7 and 95, respectively, while the CV counterparts were 6 and 75, and in both regions, the relative SNR of these two metabolites is qualitatively consistent with the differential acquisition parameters and the computed concentration ratios in these regions (Table 1).

Table 2 shows the interregional correlations of each metabolite across 19 subjects. When adjusted for multiple comparisons (see statistical methods), all correlations would be considered as trending to significant. Nevertheless, as shown in Figure 4 for Glu, the inter-regional correlation is visually compelling. Glu was the only metabolite significantly correlated across regions ($r = 0.61$, $p = 0.01$ and $p = 0.06$ when corrected for multiple comparisons). Within each region (Table 3), correlations were observed between NAA and Glu (AC: $r = 0.66$, $p = 0.06$, CV: 0.64, $p = 0.06$) (see Fig 4). Within the CV, Ins was correlated to tCh ($r = 0.63$, $p = 0.06$), NAA to tCh ($r = 0.64$, $p = 0.06$), and tCh to Glu ($r = 0.62$, $p = 0.06$), and it is noted that all metabolites are normalized to a common metabolite (tCr).

Discussion

Concentration ratios of GABA+ and Glu (in units of tCr^{-1}) were measured in the AC and CV in normal adults (n = 19, 8 males and 11 females, 24.6 +/− 6.4) with ^{1}H MRS at 3 Tesla. In addition, borderline significant intra-regional and inter-regional correlations were identified for several metabolites. Although GABA+ has not been reported from the CV using J-difference spectroscopy, ancillary metabolites are in excellent overall agreement with previous reports from regionally matched volumes. These paired measurements reflect resting state neurochemical balance in areas where proportionate dysfunction and dynamics are potentially important.

At field strengths and resolutions typical of *in vivo* MRS, GABA+ can be precisely measured only by editing its resonances from intense overlapping methyl resonances; here we use a proven pulse sequence in conjunction with post-processing quality control protocols to obtain high quality data (13). The difference spectrum between acquisitions with double selective inversions reveals coupled resonances as well as acetyl protons from NAA (13). An added benefit of this J-difference experiment and the pulse sequence parameters used in this study is that Glu resonances at 2.3 ppm are efficiently refocused and modeled without parametric baselines (Figure 2), in contrast to standard PRESS acquisitions. Reducing random and or systematic error from using basis splines to model baselines likely contributed to the inter-regional glutamate correlations observed in this study, which have not been previously observed to our knowledge.

AC GABA+ levels reported here (0.31 +/− 0.08, n= 19) cannot readily be compared to those previously reported (0.15 +/− 0.03, n = 11) (9), due to differences in acquisition and postprocessing. In the latter, basis sets for co-edited macromolecules were generated from *in vivo* acquisitions where an 800 ms inversion delay preceded the main pulse sequence. We have avoided correcting for this contaminant because acquiring *in vivo* macromolecular spectra for use as basis sets by T1-nulling is potentially prone to errors due to the absence of

suitable frequency and phase references in the corresponding spectra. Either approach certainly has merits; indeed to the extent that macromolecules are present and differ from the peaks of interest (e.g. GABA), metabolite modeling will be in error (due to incomplete prior knowledge). However, as shown in Figures 1 and 3, the GABA pseudo doublet is conspicuous and consistent across subjects, suggesting that potential overlapping resonances are remarkably similar to the GABA spectral signature.

In contrast to the AC where metabolites have been more frequently reported, edited CV GABA+ comparisons are unavailable. When referenced to tCr, CV GABA and Glu are decreased relative to the AC along with other prominent resonances in CV volumes, in accord with previous findings (20).

Glu:tCr ratios reported here (AC: 1.16 +/− 0.10, CV: 0.70 +/−0.07) agree within experimental error to recent reports. In comparable volumes, AC Glu has recently been reported in the range 1.13 – 1.21, and, in the CV, Pouwels et al have reported Glu:tCr as 0.83 +/− 0.18 using single voxel ^{1}H MRS at 2 T (21).

This study indicates that several metabolites are potentially correlated within the anterior cingulate and cerebellar vermis, but that correlations between the regions are limited to glutamate for these two areas. In all cases, the correlations are at borderline significance when adjusting for multiple comparisons, and a larger repeat study will be required to confirm these intriguing findings. Figure 4 illustrates that these correlations are conspicuous across data sets and unlikely to be driven by subsets of the data. At a cut-off of $p = 0.06$ (adjusted for multiple comparison), we found that Glu levels were linearly dependent between these regions, and that NAA was correlated to Glu within regions. In the AC, where spectral quality was increased, the correlation between NAA and Glu was unique. In the CV, four correlations were found, and it is difficult to argue that these are spurious relics of data analysis because they are observed for metabolites with high SNR and no spectral overlap (NAA and tCh, tCh and Glu). Moreover, in cases where some overlap is present (GABA and Glu), correlations are not observed. The reference to total creatine is also unlikely to explain these observations because if the denominator was driving the correlations, the effects should be observed across a broader range or the entire set of metabolites.

Conclusions

The overall quality and additional justification for using straightforward quality control measures is illustrated in Figure 3, where the complete set of AC spectra were combined. If systematic or random spectral artifacts of non-MR origin contributed to the individual spectra, it is unlikely that summed spectra would retain the features from the component spectra, which were consistent with expectations based on prior-knowledge of the spin-systems. This figure demonstrates that these data are of high quality and consistent across all acquisitions.

Given that there have been few measurements of GABA *in vivo* in AC, and none in CV, using edited ^{1}H MRS, the GABA+ concentration ratios reported here provide additional important information regarding the normative range of this inhibitory neurotransmitter in these important brain regions. While a larger database of commensurate data is necessary to build consensus on normal resting state GABA+ levels with respect to tCr in the studied regions, the overall agreement of other metabolite ratios reported here and elsewhere with distinct hardware and methods reduce the likelihood of systematic bias.

Correlations between and within these regions are potentially interesting and may enable further differentiation among disorders that involve the anterior cingulate and cerebellar vermis acting in concert. Data quality and analysis based solely on prior-knowledge enabled

the first observations of glutamate correlations between brain regions, but much more data across multiple regions will be needed to discern the specificity of these correlations and to confirm the statistical significance.

Acknowledgments

This work was supported by an NIH training grant 5T32 EB001628 entitled “Postdoctoral Training in Biomedical MRI and MRS” and an NIH Biomedical Research Partnership grant EB0000461. We thank Philips Healthcare (Best, Netherlands) for hardware and software support.

References

1. Bush G, Luu P, Posner MI. Cognitive and emotional influences in anterior cingulate cortex. Trends Cogn Sci 2000;4(6):215–222. [PubMed: 10827444]
2. Hester R, Garavan H. Executive dysfunction in cocaine addiction: evidence for discordant frontal, cingulate, and cerebellar activity. J Neuroscience 2004;24(49):11017–11022.
3. Manzardo AM, Penick EC, Knop J, Nickel EJ, Hall S, Jensen P, Gabrielli WF Jr. Developmental differences in childhood motor coordination predict adult alcohol dependence: proposed role for the cerebellum in alcoholism. Alcohol Clin Exp Res 2005;29(3):353–357. [PubMed: 15770110]
4. Minard FN, Mushahwar IK. Synthesis of gamma-aminobutyric acid from a pool of glutamic acid in brain after decapitation. Life Sci 1966;5(15):1409–1413. [PubMed: 5968706]
5. Perry TL, Hansen S, Gandham SS. Postmortem changes of amino compounds in human and rat brain. J Neurochem 1981;36(2):406–410. [PubMed: 7463068]
6. Perry TL, Hansen S, Berry K, Mok C, Lesk D. Free amino acids and related compounds in biopsies of human brain. J Neurochem 1971;18(3):521–528. [PubMed: 5559258]
7. Rothman DL, Petroff OA, Behar KL, Mattson RH. Localized 1H NMR measurements of gamma-aminobutyric acid in human brain in vivo. Proc Natl Acad Sci U S A 1993;90(12):5662–5666. [PubMed: 8516315]
8. Terpstra M, Ugurbil K, Gruetter R. Direct in vivo measurement of human cerebral GABA concentration using MEGA-editing at 7 Tesla. Magn Reson Med 2002;47(5):1009–1012. [PubMed: 11979581]
9. Bhagwagar Z, Wylezinska M, Jezzard P, Evans J, Boorman E, PMM, PJC. Low GABA concentrations in occipital cortex and anterior cingulate cortex in medication-free, recovered depressed patients. Int J Neuropsychopharmacol 2008;11(2):255–260. [PubMed: 17625025]
10. Choi C, Coupland NJ, Hanstock CC, Ogilvie CJ, Higgins AC, Gheorghiu D, Allen PS. Brain gamma-aminobutyric acid measurement by proton double-quantum filtering with selective J rewinding. Magn Reson Med 2005;54(2):272–279. [PubMed: 16032672]
11. Choi IY, Lee SP, Merkle H, Shen J. Single-shot two-echo technique for simultaneous measurement of GABA and creatine in the human brain in vivo. Magn Reson Med 2004;51(6):1115–1121. [PubMed: 15170830]
12. Oz G, Terpstra M, Tkac I, Aia P, Lowary J, Tuite PJ, Gruetter R. Proton MRS of the unilateral substantia nigra in the human brain at 4 tesla: detection of high GABA concentrations. Magn Reson Med 2006;55(2):296–301. [PubMed: 16408282]
13. Waddell KW, Avison MJ, Joers JM, Gore JC. A Practical Guide to Robust Detection of GABA in Human Brain by J-difference Spectroscopy at 3 Tesla Using a Standard Volume Coil. Magn Reson Imaging 2007;25:1032–1038. [PubMed: 17707165]
14. Mescher M, Merkle H, Kirsch J, Garwood M, Gruetter R. Simultaneous in vivo spectral editing and water suppression. NMR Biomed 1998;11(6):266–272. [PubMed: 9802468]
15. Haase A, Frahm J, Hanicke W, Matthaei D. 1H NMR chemical shift selective (CHESS) imaging. Phys Med Biol 1985;30(4):341–344. [PubMed: 4001160]
16. Bland JM, Altman DG. Calculating correlation coefficients with repeated observations: Part 2--Correlation between subjects. Bmj 1995;310(6980):633. [PubMed: 7703752]
17. Benjamini Y, Hochberg Y. Controlling the false discovery rate: a practical and powerful approach to multiple testing. Journal of the Royal Statistical Society, Series B 1995;57(1):289–300.

18. Govindaraju V, Young K, Maudsley AA. Proton NMR chemical shifts and coupling constants for brain metabolites. NMR Biomed 2000;13(3):129–153. [PubMed: 10861994]

19. Behar KL, Rothman DL, Spencer DD, Petroff OA. Analysis of macromolecule resonances in 1H NMR spectra of human brain. Magn Reson Med 1994;32(3):294–302. [PubMed: 7984061]

20. Jacobs MA, Horska A, van Zijl PC, Barker PB. Quantitative proton MR spectroscopic imaging of normal human cerebellum and brain stem. Magn Reson Med 2001;46(4):699–705. [PubMed: 11590646]

21. Pouwels PJ, Frahm J. Regional metabolite concentrations in human brain as determined by quantitative localized proton MRS. Magn Reson Med 1998;39(1):53–60. [PubMed: 9438437]

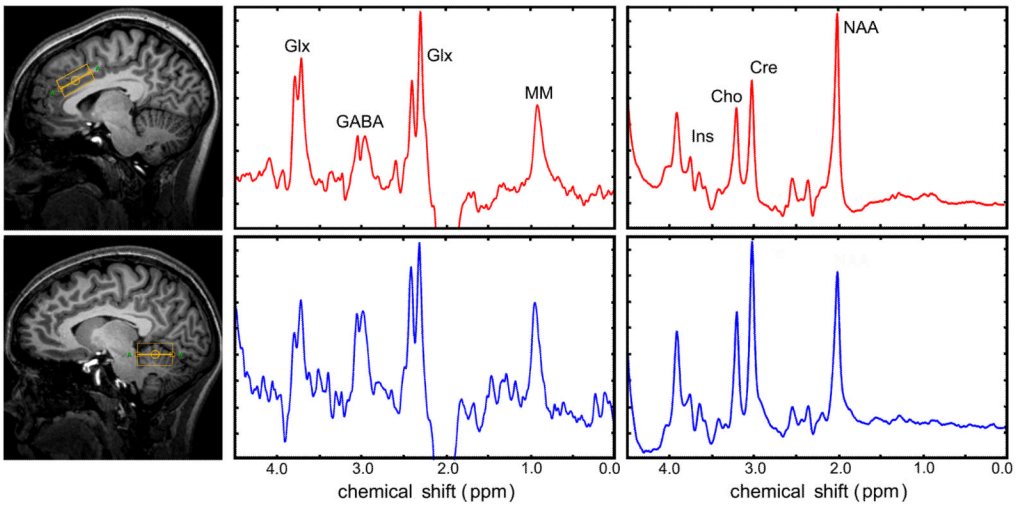

Figure 1.

Representative spectra from AC (red) and CV (blue) volumes. The left and right spectra panels correspond to J-difference and standard acquisitions, respectively. Conspicuous resonances are labeled as Glx (Glu + Gln), GABA (GABA+), Ins (myo-inositol), Cho (choline compounds), Cre (creatine methyl resonances), and NAA (N-acetylaspartate).

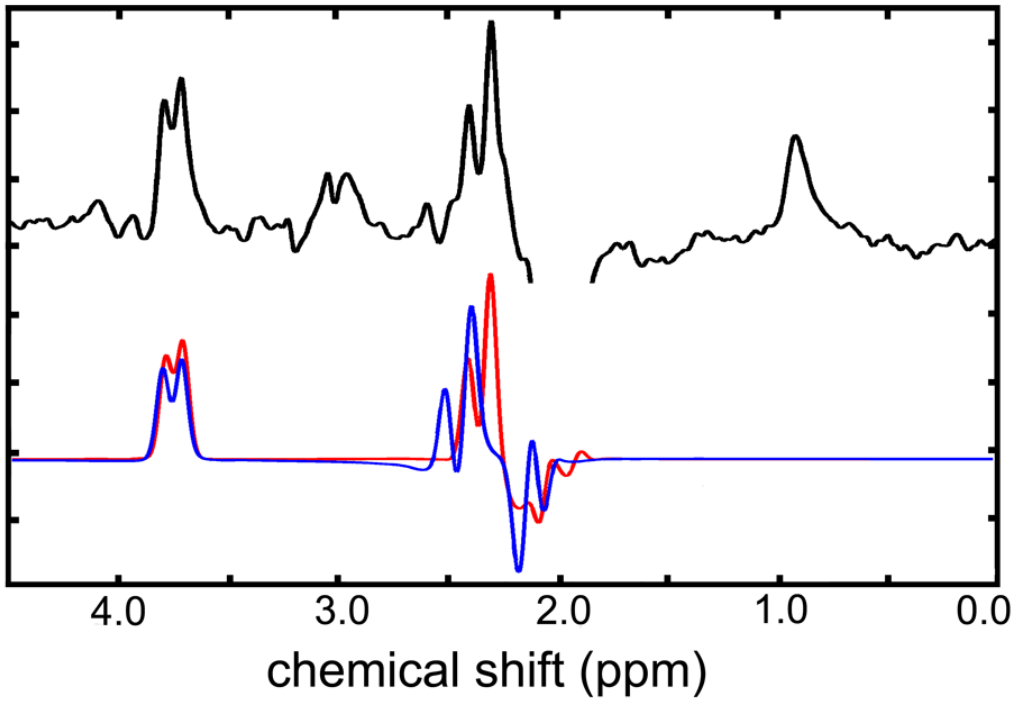

Figure 2.
Comparison of *in vivo* spectrum (upper trace) with simulated Glu (red) and Gln (blue) spectra.

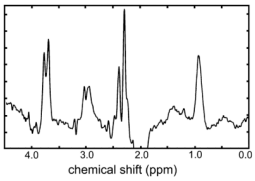

Figure 3.
Combined difference spectrum generated by summing individual spectra obtained from anterior cingulate of 19 volunteers. Individual spectra were phase and frequency corrected and summed automatically to generate this spectrum.

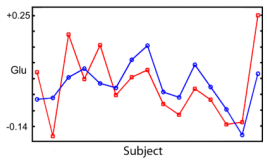

Figure 4.
Mean shifted correlations for Glu between the anterior cingulate and cerebellar vermis.

Table 1

Anterior cingulate and cerebellar vermis metabolite ratios with respect to total creatine.

	Mean	SD	Lower CI	Upper
Anterior Cingulate				
Ins	0.7048	0.0719	0.6669	0.7427
NAA	1.3319	0.0973	1.2801	1.3838
tCh	0.2434	0.0290	0.2289	0.2580
GABA	0.3130	0.0823	0.2717	0.3544
Glu	1.1605	0.1029	1.1037	1.2173
Cerebellar Vermis				
Ins	0.6913	0.0913	0.6407	0.7420
NAA	0.8002	0.0592	0.7704	0.8299
tCh	0.2278	0.0267	0.2120	0.2437
GABA	0.2288	0.0596	0.1935	0.2641
Glu	0.6965	0.0745	0.6527	0.7403

Table 2

Inter-regional correlations (anterior cingulate and cerebellar vermis).

	r	Lower CI	Upper CI	p-value	FDR*
Glu	0.6103	0.1688	0.8076	0.014	0.0583
Gaba	−0.1461	−0.5984	0.4115	0.6103	0.803
Ins	0.0339	−0.4921	0.5349	0.9064	0.9853
NAA	0.0122	−0.5062	0.5216	0.9663	0.9953
tCh	0.4154	−0.1411	0.7261	0.1256	0.3925

*Adjusted for multiple comparisons.

Table 3

Intra-regional metabolite correlations.

		r	Lower CI	Upper CI	p-value	FDR*
Anterior Cingulate						
Ins	**NAA**	0.0538	−0.4787	0.5468	0.8519	0.9853
Ins	**tCh**	0.2601	−0.3132	0.6558	0.3564	0.6731
Ins	**GABA**	0.0593	−0.475	0.55	0.8371	0.9853
Ins	**Glu**	0.047	−0.4833	0.5428	0.8705	0.9853
NAA	**tCh**	0.1729	−0.3901	0.6124	0.5452	0.7572
NAA	**GABA**	0.2447	−0.3276	0.6483	0.3869	0.6731
NAA	**Glu**	**0.6577**	0.2643	0.8272	**0.0063**	**0.0583**
tCh	**GABA**	0.2698	−0.3039	0.6604	0.3379	0.6731
tCh	**Glu**	−0.002	−0.5151	0.5129	0.9953	0.9953
GABA	**Glu**	0.2364	−0.3353	0.6443	0.4039	0.6731
Cerebellar Vermis						
Ins	**NAA**	0.3493	−0.2208	0.697	0.2065	0.5735
Ins	**tCh**	**0.6261**	0.1996	0.8141	**0.0109**	**0.0583**
Ins	**GABA**	0.2094	−0.3593	0.631	0.4616	0.7018
Ins	**Glu**	0.5644	0.0842	0.7887	0.0268	0.0957
NAA	**tCh**	**0.6426**	0.233	0.821	**0.0082**	**0.0583**
NAA	**GABA**	0.2962	−0.2777	0.6727	0.2902	0.6596
NAA	**Glu**	**0.6412**	0.2301	0.8204	**0.0085**	**0.0583**
tCh	**GABA**	0.2024	−0.3654	0.6275	0.4772	0.7018
tCh	**Glu**	**0.6193**	0.1863	0.8114	**0.0122**	**0.0583**
GABA	**Glu**	0.3018	−0.2719	0.6754	0.2805	0.6596

*Adjusted for multiple comparisons.